Quantum-trajectory analysis of an optical Stern-Gerlach experiment

Young-Tak Chough[1] and Kyungwon An[2]
[1]*Department of Applied Optics, College of Engineering, Kwangju University, Kwangju 503-703, Republic of Korea*
[2]*School of Physics, College of Natural Science, Seoul National University, Seoul 151-742, Republic of Korea*
(Received 27 November 2003; published 24 June 2004)

We present a Monte Carlo simulation of a typical cavity-QED experiment on the optical Stern-Gerlach effect in terms of the quantum trajectory method. We show that the phenomenon of wave packet splitting may be experimentally observed even in a moderate coupling regime where the atomic and cavity damping rates are comparable to the atom-field coupling strength.

DOI: 10.1103/PhysRevA.69.063817 PACS number(s): 42.50.Ct, 32.80.−t

I. INTRODUCTION

The mechanical interaction of light and matter has been comprehensively studied since the pioneering work of Kapitza and Dirac in 1933 [1]. Much work has been done on atomic beam deflection, diffraction, refraction, or interference [2–8] by a standing-wave field, classical or quantized, and the recent achievement of optical cooling and trapping of neutral atoms [9] using the light pressure force may be said to have a root in these themes. On the other hand, there were great experimental advances recently in the field of controlled single-atom or single-ion and few-photon interactions in high-Q optical cavities [10–12].

One of the interesting issues that came up in the theme of atom-field mechanical interaction is the so-called optical Stern-Gerlach effect (OSGE) [13–16]. It has been explored at various levels of sophistication since the mid-1970s when it was suggested that the trajectory of a two-state atom interacting with an optical field gradient can be split into two paths, each path containing atoms in one of the two orthogonal dressed states, under certain circumstances [15]. It is thus an optical analogy of the well-known magnetic Stern-Gerlach effect (MSGE) [17] in which the trajectory of a spin-$\frac{1}{2}$ particle is split into two paths in a magnetic field gradient.

The OSGE was experimentally demonstrated in 1992 by Sleator and others in the near-infrared ($\lambda \sim 1\ \mu$m) with metastable helium atoms (He*) [16]. The experimental result seems to be in agreement with semiclassical theories [13–15], but later it was also pointed out that the OSGE may show some additional peculiarities, sensitively depending on the quantum nature of the field [18]. Not only incorporating the quantum nature of light and the atomic center-of-mass motion in the picture, recent works also take into consideration the finite spatial extent of the atomic wave packet [19–21], rather than treating an atom as a point mass [3] or a plane wave [13,14] in space. References [22,23] deal with the OSGE on resonance with quantized light field, whereas the Refs. [24,25] treat the case of off resonance although the wave packet is limited to quadratic and linear sections of the optical potential. Particularly, the first reference in [19] presents quite an elegant operator method in such a full quantum-physical description of the OSGE.

Noting, however, that the theories originally envisaged the OSGE as coherent processes dealing with ideal lossless systems, mostly in the linear regime, we explored the role of decoherent processes in the OSGE, particularly in the nonlinear regime, which may be significant in the optical frequencies. For systems free of damping, decent analytic treatments may be available, but when the system is open to its environment so that the coherent dynamical evolution of the system is frequently interrupted by discontinuous processes such as atomic spontaneous decays or cavity emissions, etc., analytic approaches may not be always possible. There are a number of theoretical methods to deal with such open quantum systems, but we resorted to the quantum trajectory theory (QTT) [26] with our 16-node PC cluster (CPU clock speed 2.4 GHz/node). Along with the numerical work, we analyzed as well the effect of damping in the dynamics of atomic wave packets in the quantum-trajectory point of view.

In Sec. II, we first provide our simple anad intuitive illustration [27] on the OSGE, based on the dressed-state picture [28], and in Sec. III, we discuss the effect olf damping in the language of QTT. In Sec. IV, we perform a numerical simulation of a typical experiment one can practically set up. Section V summarizes this work.

II. OPTICAL STERN-GERLACH EFFECT

A. Wave packet "pulsation"

Consider a simple model in which a Gaussian wave packet of a two-state atom initially in its ground state is placed on a node of a standing-wave cavity, on the cavity axis, as illustrated in Fig. 1. In order to quickly appreciate

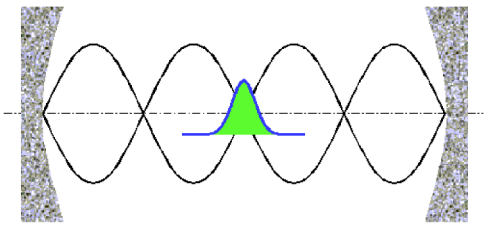

FIG. 1. The model. The Gaussian wave packet of a two-state atom initially in its ground state is placed on a node of a standing-wave cavity, on the cavity axis.

the essential physics, let us assume that the cavity field is initially in a single-quantum Fock state, and the atom and cavity are on resonance. We will neglect damping for the time being. The interaction Hamiltonian is then simply written as

$$H = \frac{p^2}{2M} + i\hbar g(x)(\sigma_- a^\dagger - \sigma_+ a), \tag{1}$$

where p is the atomic momentum operator conjugate to the position x on the cavity axis, M the atomic mass, and $g(x)$ the atom-field coupling strength at position x such that

$$g(x) = g_0 \sin kx, \tag{2}$$

g_0 being a constant and k the field wave number. $a^\dagger$ (a) is the creation (annihilation) operator for the field, and $\sigma_+ = |e\rangle\langle g| = (\sigma_-)^\dagger$ is the atomic excitation operator, with e (g) labeling the atomic excited (ground) state.

We will focus only on a spatially well-localized wave packet such that its initial width Δx is much smaller than the wavelength λ of the cavity field. We choose $\Delta x = \lambda/40\pi$ which corresponds to the width in momentum space, $\Delta p = 10\hbar k$ [29]. Due to the finite spatial extent of the wave packet, the atom-field coupling strength at the node is nonzero, although very small compared to its peak value g_0, and the interaction slowly commences. Note that the initial effective coupling strength is given by an overlap integral of the mode function and the atomic spatial probability distribution—i.e.,

$$\begin{aligned} g_{\text{eff}} &= \int dx \psi_0^2(x)|g(x)| \\ &= 2\int_0^\infty \frac{1}{\sqrt{2\pi(\Delta x)^2}} \\ &\quad \times \exp\left[-\frac{x^2}{2(\Delta x)^2}\right] g_0 \sin kx\, dx \\ &\sim 2\sqrt{2\pi}\left(\frac{\Delta x}{\lambda}\right) g_0 \\ &\sim 0.04 g_0, \end{aligned} \tag{3}$$

where $\psi_0(x)$ is the initial atomic wave packet and we put $\sin kx \sim kx$ as $\Delta x \ll \lambda$. Thus the effective coupling strength would be only about 4% of g_0 initially.

Let us first present our numerical results on the evolution of the atomic wave packet in Figs. 2(a) and 2(b). Precisely speaking, the figures show the position and momentum distributions which are nothing but the mod squares of the wave packet in the position and momentum representation, respectively. Details of the numerical work are given in Sec. III. Note that since the atomic mass M, field wave number k, and atom-field coupling constant g_0 appear in the Hamiltonian at the same time, one needs to specify these quantities somehow, but the only system-dependent parameter is the dimensionless factor $\mu = \hbar k^2/2Mg_0$, which appears from the Schrödinger equation when we rescale time in units of g_0^{-1} and the momentum in $\hbar k$. Note that $\mu = k(\hbar k/M)/2g_0$

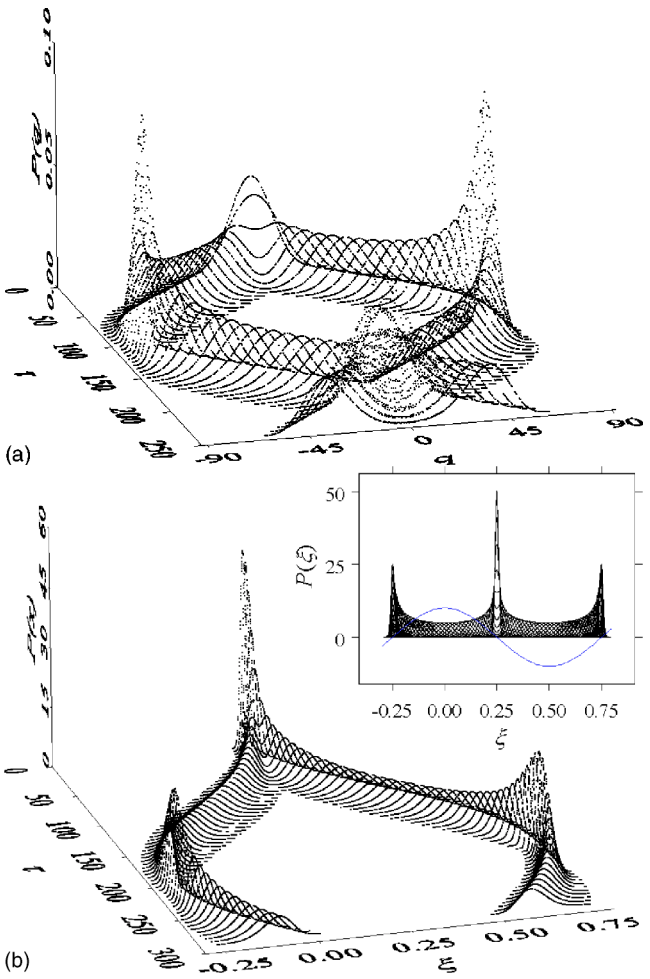

FIG. 2. The evolution of an atomic wave packet placed on a node of the cavity field. The probability distributions in momentum space (a) and in coordinate space (b). $q = p/\hbar k$, $\xi = x/\lambda$, and $\tau = g_0 t$. For a typical atom with $\mu = \hbar k^2/2Mg_0 \sim 1.7 \times 10^{-4}$. The atom is initially in the ground state having a momentum spread $\Delta p = 10\hbar k$ while the field is prepared in a single-quantum Fock state. The inset is a lateral view of (b) into the time axis along with the $\cos kx$ curve.

$= kv_1/2g_0$ is the ratio of the Doppler shift by the single-photon recoil to the single-photon Rabi frequency. Let us take $\mu = 1.7 \times 10^{-4}$ with $M = 100$ a.u., $\lambda = 600$ nm, and $g_0 = 200$ MHz for a typical atom interacting with an optical field in the strong coupling regime.

The figures show that the initial Gaussian packet evolves into a double-peaked distribution and then back to its original shape, as time proceeds. The inset is a ground-level view of the packet in the coordinate space along with the $\cos kx$ curve, which clearly shows that the two split bumps make turns exactly at the neighboring nodes. Let us first note that the two figures are *mechanically* consistent in the following sense. Let $\tau = g_0 t$. In momentum space, the position $\overline{p}$ of one of the split peaks grows roughly linearly in time in the fashion $\overline{p}(\tau) \sim 0.9\hbar k\tau$ until $\tau \sim 100$ and then bounces back to the original position. So the position $\overline{x}$ of a peak after one cycle of motion in momentum space is roughly

$$\overline{x} \sim 2\int_0^{100/g0} \frac{\overline{p}}{M} dt \sim (2.9 \times 10^3 \mu)\lambda = 0.49\lambda - 0.5\lambda, \quad (4)$$

which is in a good agreement with Fig. 2(b). Although this wave packet motion can be said to have essentially a quantum-mechanical origin in the sense that $\overline{x}$ vanishes if $\hbar$ does, the motion conforms at the same time to classical mechanics. We will get back to this apparently trivial observation when we include damping in the system in Sec. II and will point out some interesting features in connection to this issue.

Thus we have seen an exotic phenomenon of *wave packet pulsation on a node*. Notice that since the atom and cavity are on exact resonance, there is *no* net dipole force [28] as it is proportional to the atom-cavity detuning. So this phenomenon does not seem to be explained in terms of the dipole force. For a quick comparison, Ref. [30], for instance, discusses the atomic dynamics in the large detuning limit. In this limit, the atom will stay essentially in its ground state all the time, and consequently there will be no significant wave packet dispersion. Thus the atomic motion can be well approximated to that of a classical oscillator moving in a *nonzero* dipole force field and is conceptually easy to understand.

Note also that the analytic approaches such as [19] based upon the linear approximation did not predict this *pulsation*. The descriptions are mostly limited to the wave packet splitting in an early stage of the atom-field interaction. If the atoms are let to leave the interaction region at some point of time, the emerging wave packet will have a pair of distinguishably separated probability density peaks. This phenomenon of wave packet splitting is the very optical Stern-Gerlach effect mentioned in the Introduction. In the following, let us provide a simple intuitive account for the physical origin of the wave packet pulsation that we have just seen, in the viewpoint of the dressed-state picture [28].

B. Dressed-state picture, on resonance

Dressed states are the eigenstates of the atom-cavity combined system which form a manifold of infinite hierarchy called the Jaynes-Cummings ladder. Since only one quantum is in the system, we need only to consider up to the first couplet such that

$$|\pm\rangle = (1/\sqrt{2})(|0,e\rangle \pm i|1,g\rangle), \quad (5)$$

which have Rabi-split eigenenergies given by

$$E_\pm(x) = \hbar[\omega_0 \pm g_0 \sin(kx)], \quad (6)$$

where 0 and 1 count the number of quanta in the field. Figure 3(a) shows the spatial variation of $E_\pm(x)$ on the cavity aris around a node. In the figure, one can immediately see that if the system is in state $|+\rangle$, it will start to slide down the slope of its energy curve and move to the left, and in $|-\rangle$, to the right. However, as one can easily show, the state function of the system at an arbitrary time turns out to be always a 50-50 superposition of $|+\rangle$ and $|-\rangle$ when the system starts out in an energy eigenstate—e.g., $|1,g\rangle$. Thus, half of the wave packet sitting on a node is pushed to the left and the other half to the right, resulting in the splitting of the packet into two pieces. When the two split bumps of wave packets hit the turning points at the neighboring nodes, they return just like a pair the of classical particles. This is the essential explanation as to why we have such a pulsation of the wave packet as in Figs. 2(a) and 2(b). We can do a very simple Newtonian mechanics here again. One of the two components of the wave packet will receive from the energy slope a force of size $F=\hbar k g_0 \cos kx$. In the early stage of time where a linear approximation is valid, $F \sim \hbar k g_0$ and the peak will gain the momentum growing as $\overline{p} \sim \hbar k \tau$ initially. But the overall behavior is rather close to our eye estimation of $\overline{p}(\tau) \sim 0.9\hbar k\tau$ in Eq. (4). One can easily show that the period τ_0 of the wave packet pulsation in coordinate space is exactly given by $\tau_0 = (2/\sqrt{\mu})\int_0^{\pi/2} ds/\sqrt{\sin s} \approx 400$; cf. Fig. 2(b).

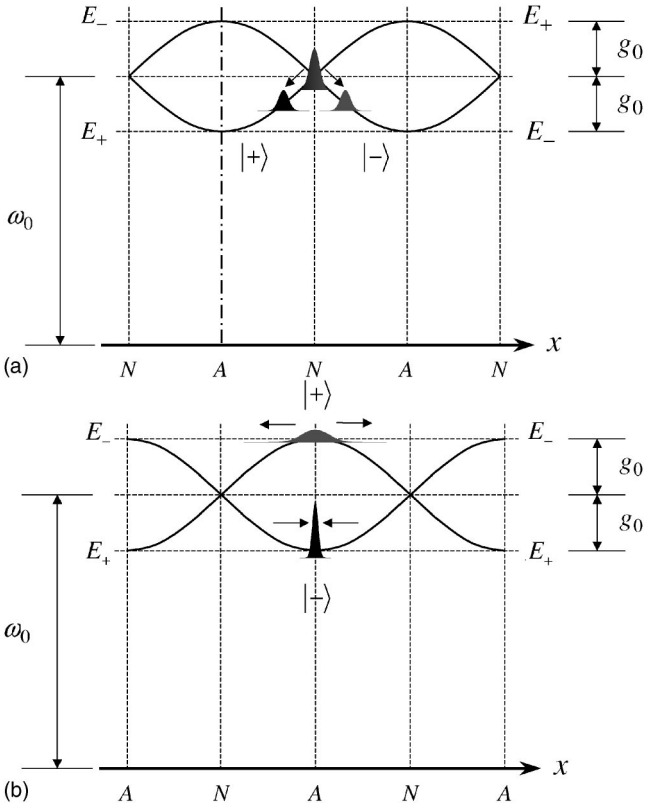

FIG. 3. Spatial modulation of the dressed energies ($\hbar=1$) and motion of the dressed states starting from a node (a) and from an antinode (b). *A* and *N*, respectively, denote antinode and node.

In this fashion, the dressed-energy gradient created by the nonuniform spatial structure of the cavity field plays as a dressed-state selector, splitting the atomic wave packet into two distinct groups of orthogonal dressed states, $|+\rangle$ and $|-\rangle$, which is the very OSGE. Let us add that, on an antinode, on the other hand, the $|+\rangle$ component of the wave packet tends to be pulled out to both sides of the antinode while the $|-\rangle$ component tends to be squashed toward the antinode as illustrated in Fig. 3(b), giving the net effect of distorting the initial Gaussian packet into a wing-broadened, peak-sharpened feature.

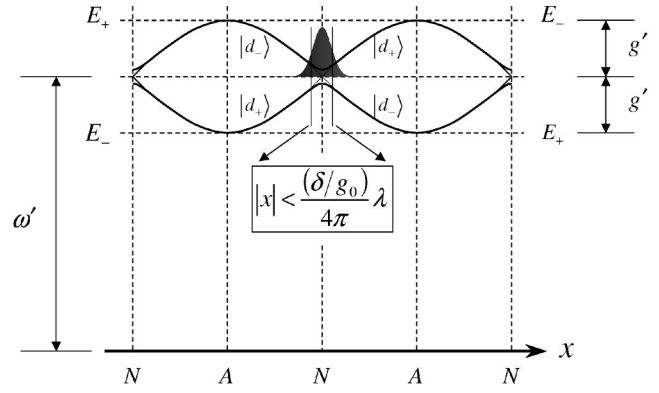

FIG. 4. Spatial modulation of the dressed energies ($\hbar=1$) in the presence of nonzero atom-field detuning. $\omega'=\omega_0+\delta/2$ and $g'=\sqrt{g_0^2+(\delta/2)^2}$.

C. Off-resonant case

In the actual experiments, however, it is not practically possible to keep the *exact* resonance indefinitely. So let us consider the case in which the atom and cavity are slightly detuned. Let $\delta\equiv\omega_C-\omega_A$ denote the detuning, where $\omega_{A(C)}$ is the atomic transition (cavity resonance) frequency. The atom-cavity detuning causes an anticrossing of the energy levels which makes the picture slightly complicated. The first couplet is now designated by

$$|d_+\rangle = \cos\theta|0,e\rangle + i\sin\theta|1,g\rangle, \tag{7a}$$

$$|d_-\rangle = \sin\theta|0,e\rangle - i\cos\theta|1,g\rangle, \tag{7b}$$

where

$$\tan\theta = [\delta/2g(x)] + \sqrt{[\delta/2g(x)]^2+1}, \tag{8}$$

with the associated eigenenergies given by

$$E_1^{\pm}(x) = \hbar[\omega_0+(\delta/2)] \pm \hbar\sqrt{g^2(x)+(\delta/2)^2}, \tag{9}$$

as depicted in Fig. 4 [28]. One has to be careful about the association of the eigenenergies to the eigenstates. In the region where $X\equiv\delta/2g(x)$ is positive, $|d_\pm\rangle$ are associated with $E_1^{\pm}$, but in the negative X region, these are associated with $E_1^{\mp}$. This is simply because $\sin\theta|_{\pm X}=\cos\theta|_{\mp X}$ (due to the mutually symmetric behavior of $\sin\theta$ and $\cos\theta$ around $\theta=\pi/4$), and the eigenenergies are determined by the mod squares of the coefficients—i.e.,

$$\begin{aligned} E_+ &= |\cos\theta|^2\hbar\omega_a + |\sin\theta|^2\hbar\omega_c \quad \text{for } X\geqslant 0 \\ &= |\sin\theta|^2\hbar\omega_a + |\cos\theta|^2\hbar\omega_c \quad \text{for } X<0, \end{aligned} \tag{10}$$

etc. It is sufficient to consider the solution of Eq. (8) in the range $0\leqslant 2\theta\leqslant\pi$. Let us first consider two limiting cases. First, in the regions relatively far from the node where $|X|\ll 1$, we have $\theta\to\pi/4$, and therefore $|d_\pm\rangle$ respectively approximate to $|\pm\rangle$. Thus, in these regions, the wave packet behaves just like in the case of exact resonance discussed above, as expected. Note that, on the left-hand side of the node, $|d_+\rangle$ has the lower energy $E_1^-(x)$, which approaches $E_+(x)$ in Eq. (6), and $|d_-\rangle$ the higher energy $E_1^+(x)\approx E_-(x)$, whereas on the right-hand side, the levels are reversed. Second, in the region near the node, on the other hand, we have $\delta/2g(x)\to\pm\infty$. When $g(x)$ approaches the node from the positive side, $\theta\to\pi/2$ and when it approaches from the negative side, $\theta\to 0$. Thus the behavior of the first couplet is summarized as

$$\begin{array}{lll} & g(x)<0 & g(x)>0 \\ E_1^+: & |d_-\rangle\to|1,g\rangle & |d_+\rangle\to|1,g\rangle, \\ E_1^-: & |d_+\rangle\to|0,e\rangle & |d_-\rangle\to|0,e\rangle, \end{array} \tag{11}$$

What it means is the following: if the system is in $|1,g\rangle$, for instance, the system is placed in a potential well defined by $E_1^+(x)$ in this region, and when it is in $|0,e\rangle$, it is sitting on a potential hill defined by $E_1^-(x)$. Thus, if the system starts from $|1,g\rangle$, the portion of the wave packet in this region tends to be trapped in the potential well of $E_1^+(x)$ while the wings of the packet outside this central region will slide down the slopes of $E_1^-(x)$ on both sides of the node, since outside the region, $|1,g\rangle$ is a combination of $|d_\pm\rangle\approx|\pm\rangle$ as a aforementioned. Note that the overall state of the system at arbitrary time is no longer a 50–50 combination of $|d_\pm\rangle$. Nevertheless, the packet motion occurs always in a symmetric fashion about the node, as a matter of course. To see this, write the internal state as $|\psi\rangle=C_1|0,e\rangle+C_2|1,g\rangle$ with complex coefficients C_1 and C_2. Then, at a position $x=x_1$ (with respect to the origin at a node), it is written as $|\psi\rangle=A_+|d_+\rangle+A_-|d_-\rangle$ where $A_+=C_1\cos\theta-iC_2\sin\theta$ and $A_-=C_1\sin\theta+iC_2\cos\theta$, whereas at $x=-x_1$, it is given by $|\psi\rangle=B_+|d_+\rangle+B_-|d_-\rangle$ where $B_+=C_1\sin\theta-iC_2\cos\theta$ and $B_-=C_1\cos\theta-iC_2\sin\theta$. But since $|A_\pm|=|B_\mp|$, the portions of the wave packet in the upper energy state on both sides are the same. Thus the symmetry arises around the node. The ratio of the portions in the upper and lower energy states, however, is changing in time. As a result, we will have the initial single-bumped wave packet evolving into a *triple*-peaked structure on a node in the presence of finite atom cavity detuning instead of the double-peaked shape in case of the exact resonance.

Our expectation is nicely confirmed by a numerical calculation as shown in Fig. 5 where we take $\delta/g_0=0.1$, for instance, with other parameters the same as before. Of course due to the small effective coupling constant, the system slowly evolves from $|1,g\rangle$ to $|0,e\rangle$, and the portion of the wave packet in the central region will also gradually migrate into both sides of the node. The volume of the central region is confined by $|(2g_0/\delta)\sin(kx)|\ll 1$ or $|x|/\lambda\ll(1/4\pi)(\delta/g_0)$. For $\Delta x/\lambda=1/40\pi$ we have $|x|/\Delta x\ll 10(\delta/g_0)$. If $\delta/g_0\sim 0.01$, then $|x|/\Delta x\ll 0.1$, which implies, though loosely, that by far the largest part of the wave packet resides outside this region and the central peak wil not be significant if $\lambda/g_0\leqslant 0.01$.

Let us leave a brief note regarding the dependence on the field state. If the field state includes a nonzero amplitude of the vacuum state $|0\rangle$ as in the case of a coherent state, this portion of field will tend to leave the atomic wave packet intact in time. So there will be always some portion of the packet standing still at its original position. This will show

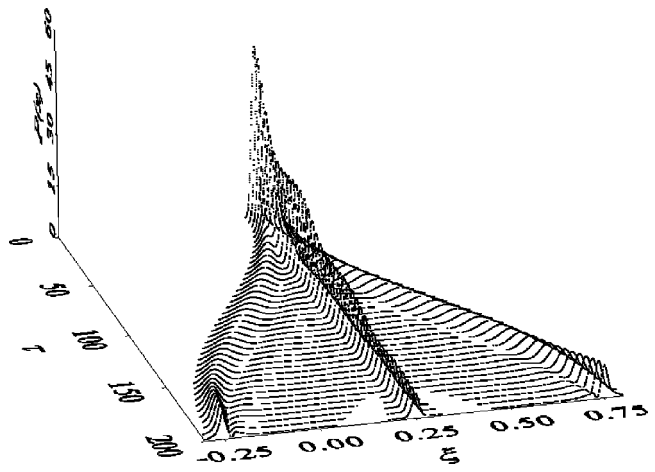

FIG. 5. Wave packet evolution in coordinate space in the presence of nonzero atom-field detuning, $\delta/g_0=0.1$, while other parameters are the same as in Fig. 2. $\xi=x/\lambda$.

up as a peak at the center between the two separate peaks on both sides, making the overall look of the wave packet somewhat similar to the case of nonzero detuning aforementioned. This fact is most easily seen in the Schrödinger picture. We will get back to this point at an appropriate place in the next section since we will explicitly deal with the Schrödinger equations there.

III. OSGE IN THE PRESENCE OF DAMPING

The picture given so far in the dressed-state formalism provided a qualitative but intuitive understanding of the phenomenon. Nevertheless, the real systems are after all *open* quantum systems subject to damping, and the dynamical effects of such decoherent processes are yet to be discussed. The open systems can be dealt with in a number of ways—e.g., master equations [26,31], quantum Langevin equations [31], or Fokker-Planck equations [31,32] in appropriate situations. In this work, we deal with the system in the viewpoint of the quantum-trajectory theory [26], doing the numerical work with our 16-node PC cluster of clock speed 2.4 GHz. Below, we will analyze rather in detail how QTT describes the time evolution of an atomic wave packet, particularly at the events of spontaneous emissions as the atom is moving through a node of the field.

A. Quantum trajectory formulation

A quantum trajectory consists of piecewise continuous coherent evolution and discontinuous jumps such as the atomic and cavity decays which randomly interrupt the coherent evolution. Let Γ_i $(i=1,2,\ldots)$ denote the various decay rates in the system and C_i the corresponding "collapse" operators—e.g., σ_- for the atomic emission and a for the cavity transmission. Then the coherent evolution of the system is given by the following Schrödinger-like equation:

$$i\hbar\frac{d}{dt}|\overline{\Psi}\rangle=\left(H-\sum_i i\hbar\frac{\Gamma_i}{2}\mathcal{C}_i^\dagger\mathcal{C}_i\right)|\overline{\Psi}\rangle. \tag{12}$$

Thus the Schrödinger process is slightly modified by the damping terms. Because of the damping terms, it is not a norm-conserving process, and $|\overline{\Psi}\rangle$ represents an *unnormalized* wave function. When the collapse probability

$$p_c^i=\Gamma dt\frac{\langle\overline{\Psi}|\mathcal{C}_i^\dagger\mathcal{C}_i|\overline{\Psi}\rangle}{\langle\overline{\Psi}|\overline{\Psi}\rangle} \tag{13}$$

is greater than a random number $R\in[0,1)$ taken during the time interval $[t,t+\mathrm{d}t)$, a quantum jump occurs in the fashion

$$|\overline{\Psi}\rangle\rightarrow\mathcal{C}_i|\overline{\Psi}\rangle. \tag{14}$$

Otherwise, the system dynamics follows Eq. (12). For further details of the theory, see, e.g., [26].

Now let us return to the original problem in which an atomic wave packet in its ground state is placed at a node of the cavity field mode, on the axis of the cavity. The cavity can contain any photonic state of light, and let us neglect cavity damping ($\kappa=0$) for the time being in order to focus on the effect of atomic damping. For algebraic convenience, let us write $g(x)=g_0\cos(kx)$ and assume a very massive atom so that the kinetic energy term can be neglected (Raman-Nath approximation). Then the Hamiltonian in the interaction picture becomes as simple as

$$H=i\hbar g_0\cos(kx)(\sigma_-a^\dagger-\sigma_+a). \tag{15}$$

We expand the wave function in the fashion

$$|\overline{\Psi}\rangle=\int dq\left\{\sum_{n=1}^{\infty}[\overline{C}_e(n,q)|n-1,q,e\rangle+\overline{C}_g(n,q)|n,q,g\rangle]+\overline{C}_g(0,q)|0,q,g\rangle\right\}, \tag{16}$$

where n is the field quantum number and q the atomic momentum quantum number scaled in unit of $\hbar k$. The coherent evolution is then given by the following set of dynamical equations:

$$\frac{d}{d\tau}\overline{C}_e(n,q)=-\frac{\sqrt{n}}{2}[\overline{C}_g(n,q-1)+\overline{C}_g(n,q+1)]-\frac{\gamma}{2}\overline{C}_e(n,q)\quad(n\geqslant 1), \tag{17a}$$

$$\frac{d}{d\tau}\overline{C}_g(n,q)=+\frac{\sqrt{n}}{2}[\overline{C}_e(n,q-1)+\overline{C}_e(n,q+1)]\quad(n\geqslant 0), \tag{17b}$$

where we used the relations $\cos(kx)=(1/2)[\exp(ikx)+\exp(-ikx)]$ and $\exp(\pm ikx)|q\rangle=|q\pm1\rangle$ with $\tau=g_0t$ and $\gamma=\gamma_A/g_0$ the atomic decay rate scaled in g_0. So the nth Jaynes-Cummings couplet is decoupled in dynamics from the rest of the infinite hierarchy of couplets.

The state of the cavity field $|\psi_\mathrm{f}\rangle$ can be expressed as a linear combination of the number states—i.e.,

$$|\psi_f\rangle = \sum_n f(n)|n\rangle. \tag{18}$$

Let the initial atomic position $x=\xi_0\lambda$ and the momentum spread $\Delta p=(\Delta q)\hbar k$. Then the initial wave packet is given by

$$|\Psi(0)\rangle = \int dq \sum_{n=0}^{\infty} \exp\left[\frac{-q^2}{4(\Delta q)^2}\right]\exp(-2\pi i q\xi_0)F(n)|n,q,g\rangle, \tag{19}$$

where $F(n)$ denotes the normalized coefficients such that

$$F(n) = \frac{1}{\sqrt[4]{2\pi(\Delta q)^2}} f(n). \tag{20}$$

The initial values are therefore

$$C_e^0(n,q) = 0 \quad (n \geqslant 1), \tag{21a}$$

$$C_g^0(n,q) = F(n)\exp\left[\frac{-q^2}{4(\Delta q)^2}\right]\exp(-2\pi i q\xi_0). \tag{21b}$$

Now at a node, $\xi_0=1/4$, and Eq. (21b) is written as

$$C_g^0(n,q) = F(n)e^{-\beta q^2}e^{-i(\pi/2)q}, \tag{22}$$

where $\beta=1/4(\Delta q)^2$, being the width parameter of the initial wave packet. With this initial value, we solve Eqs. (17a) and (17b) in the Eulerian fashion such that

$$\overline{C}_{e(g)}^{\nu d\tau}(n,q) = \overline{C}_{e(g)}^{(\nu-1)d\tau}(n,q) - d\tau\dot{\overline{C}}_{e(g)}^{(\nu-1)d\tau}(n,q), \tag{23}$$

where time τ is divided by small discrete steps $d\tau$ so that $\tau = \nu d\tau$ with an integer ν. We obtain the behavior of the system at an early time τ given by

$$\overline{C}_e^{\tau}(n,q) \sim -iC_g^0(n,q)\left(\frac{\tau\sqrt{n}}{2}\right) \times[e^{\beta(2q-1)} - e^{-\beta(2q+1)}]e^{-(\gamma/2)\tau} \quad (n \geqslant 1), \tag{24a}$$

$$\overline{C}_g^{\tau}(n,q) \sim C_g^0(n,q)\left\{1 + \frac{3}{8}\left(\frac{\tau\sqrt{n}}{2}\right)^2 \times[e^{4\beta(2q-1)} - 2 + e^{-4\beta(q+1)}]\right\} \quad (n \geqslant 0), \tag{24b}$$

keeping terms up to the order of $(d\tau)^2$. Note that by comparing with the numerical solutions, we find that these expressions are valid up to $\tau\sim 5$. If the damping is weak, there will be little difference in the coherent evolution in early times such that $\exp(-\gamma\tau/2)\approx 1$. But what it does in the jump process is quite remarkable. Since now there is a small probability built up that the atom is in the excited state, there is a probability that the atom will decay. Let us just assume that such a decay happened now. The wave packet then undergoes a quantum jump such that

$$|\overline{\Psi}\rangle \to \exp(-ikx\eta)\sigma_-|\Psi\rangle, \tag{25}$$

where $\exp(-ikx\eta)$ describes the momentum recoil that the atom gets from the emission, projected on the x axis, and η is a random number in the range $[-1,1]$. Here $|\bar{\bar{\Psi}}\rangle$ represents an unnormalized wave function. In the coefficients, this process is written as

$$\overline{C}_e^{\tau}(n,q) \to 0, \tag{26a}$$

$$\overline{C}_e^{\tau}(n,q) \to \overline{C}_e^{\tau}(n+1,q+\eta) \propto F(n+1) \times[e^{-\beta(q+\eta-1)^2} - e^{-\beta(q+\eta+1)^2}]e^{-(\gamma/2)\tau}. \tag{26b}$$

Since then, the entire wave packet is determined by $\overline{C}_g^{\tau}(n,q)$, yielding the probability distribution in momentum space such that

$$\mathcal{P}(q) = \sum_n |C_g^{\tau}(n,q)|^2 \propto [e^{-\beta(q+\eta+1)^2} - e^{-\beta(q+\eta-1)^2}]^2. \tag{27}$$

It is simply the square of the difference of two Gaussians which are slightly shifted from each other. So obviously it will show a *double*-peaked structure. The locations of the extrema of $\mathcal{P}(q)$ are easily found in the limit of small β. Note that we are considering a spatially well-localized atomic wave packet ($\Delta x \ll \lambda$) to which the small-β limit applies. Then the locations of the two bumps in $\mathcal{P}(q)$ are given by $q \approx \pm\sqrt{2}(\Delta q)(|\eta| \ll \Delta q)$. Thus the initial momentum spread somehow determines the locations of the peaks in the split wave packet in the early stage of the atom-field interaction.

Figures 6(a) and 6(b) show the shapes of the wave packet (again, the probability distribution, indeed) of an atom sitting on a node right after an atomic jump that is arranged to occur at a few different times, in the early stage of the atom-field interaction: (a) in momentum space and (b) in coordinate space, at various times of the atomic jump, $\tau=1, 2, \ldots, 5, 10$, and 20, with the same set of parameters as in Figs. 2(a) and 2(b). The Gaussian curve is the initial packet. Note that the curves are independent trajectories. The figures show that our simple argument reaching Eq. (27) is quite valid up to $\tau\sim 5$. It is seen that in coordinate space, the longer the coherent evolution time elapsed before the jump, the narrower both the widths of and the separation between the split peaks become, whereas in momentum space, the wider both become.

In fact, one can extract two separate dynamical mechanisms at work in these pictures. First, the packet splitting in coordinate space—or in other words, the fact that $\mathcal{P}(\xi)=0$ at a node—right after an atomic jump has the following physical grounds. The event of an atomic jump implies that the atom was in the excited state before the jump. For the atom

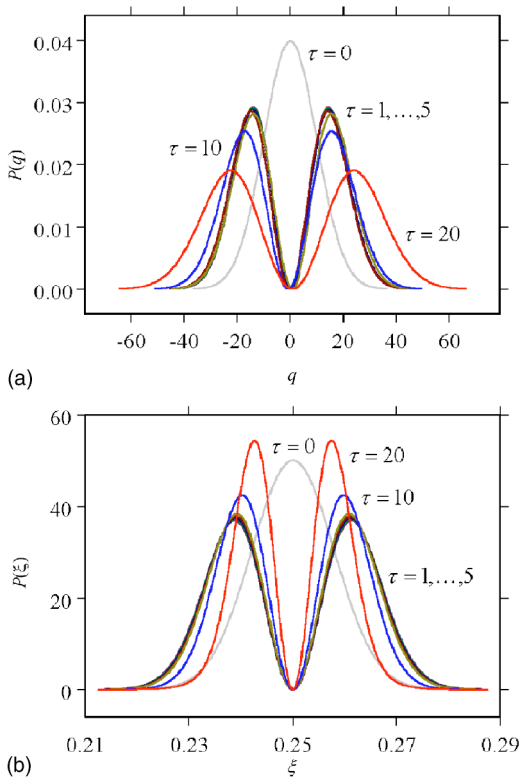

FIG. 6. The shapes of the wave packet sitting on a node right after an atomic jump arranged to occur at $\tau=1,\ldots,5,10$, and 20 (a) in momentum space and (b) in coordinate space. $q=p/\hbar k$, $\xi=x/\lambda$.

to be lifted from its initial ground state to the excited state, the atom-field interaction must be nonzero. So an event of the atomic jump tells us that the probability for the atom to be at the node was indeed zero, and our initial Gaussian wave packet has been accordingly modified through the backaction of the measurement. Second, the reason that the separation of the two split peaks in coordinate space becomes smaller and smaller as the advent of the atomic jump is delayed is explained in the same context. That is, if the atomic jump has not occurred after all, we have to conclude that actually the atom has not gone through the Rabi interaction with the cavity field and has stayed in the ground state. This means that the wave packet becomes narrower and narrower around a node as time goes by before an atomic jump really occurs. When a jump occurs, the packet is split into two through the first mechanism, but since the separation of the split packet is determined by the width of the packet before the jump, it is narrower also. Thus one may add that the theory of the quantum trajectory is none other than the process of a continuous correction of our "lack of knowledge" about the state of the system, based upon the information provided from the measurements. The measurements here are of course made by the environment—i.e., the vacuum field which is continuously monitoring the atomic damping.

The irregular shifts of the packets in momentum space are due to the random momentum recoils from the atomic spontaneous emissions, whereas no such shifts are shown in coordinate space. Note, however, that the latter is *not* because the atomic mass is infinite, but simply because

$$|\psi_1(x)|^2 = \left| \int dp\varphi(p-p_1)\exp(ipx/\hbar) \right|^2 = \left| \int dp\varphi(p)\exp(ipx/\hbar) \right|^2 = |\psi_0(x)|^2, \tag{28}$$

regardless of the size of the recoil momentum p_1 or the atomic mass—for the dual wave functions $\psi(x)$ and $\varphi(p)$. The physical reason for this is that the atomic jump has been assumed to occur *instantaneously*; i.e., no time has elapsed before and after the jump. Hence no displacement before and after the momentum kick. However, the absence of motion in the coordinate space *between* the atomic jumps is due to the infinity of the atomic mass. As a matter of course, when the atomic mass is finite, the system will evolve in coordinate space *after* an atomic jump according to the momentum kick that it has gained. Anyhow, we see that there is some "internal motion," if we may, i.e., splitting, spreading, and separation, of the wave packet even for an *infinitely* massive atom in an optical cavity although there is no center-of-mass motion. This interesting feature seems to deserve some further discussion. The following subsection is devoted to this purpose.

B. "Dynamics" of an *infinite* mass

Although an atom with infinite mass is entirely a fictitious object, it deserves a consideration at this moment as it provides a deeper understanding of the quantum-trajectory point of view. We just see that the wave packet of an infinitely heavy atom interacting with the cavity field does show dynamics in momentum space, which is of course due to the momentum exchanges with the field. In coordinate space, however, nothing happens *provided* that the system is free of damping, *no matter what happens to the wave packet in momentum space*, as shown in Figs. 7(a) and 7(b). In the figure, the inset is a lateral view of the three-dimensional-plot on the bottom from the time axis which clearly shows the time invariance of $\mathcal{P}(\xi)$, the probability distribution in coordinate space. From the viewpoint of mechanics, it appears rather understandable as the atomic mass is assumed to be infinite, but is still quite interesting in the sense that $\mathcal{P}(\xi)$ is essentially (though not exactly) a Fourier-type transform of $\mathcal{P}(q)$. So, if $\mathcal{P}(q)$ changes so radically as shown in Fig. 7(a), one would naively expect some change in $\mathcal{P}(\xi)$ also, whatever it may be.

If we write the wave packet in the same fashion as Eq. (16), $\mathcal{P}(\xi)$ at time t is given by

$$\mathcal{P}(\xi) = \mathcal{P}_0 \sum_{n,a} |dq e^{i2\pi q\xi} C_a(n,q)|^2, \tag{29}$$

where a labels the atomic internal states and $\mathcal{P}_0$ a normalizing constant. The coefficients $C_a(n,q)$ continuously evolve in time with the Hamiltonian, Eq. (15), but only in such a fashion that $\mathcal{P}(\xi)$ remains invariant in time. This is in fact easily proved by looking at the time derivative of $\mathcal{P}(\xi)$—i.e.,

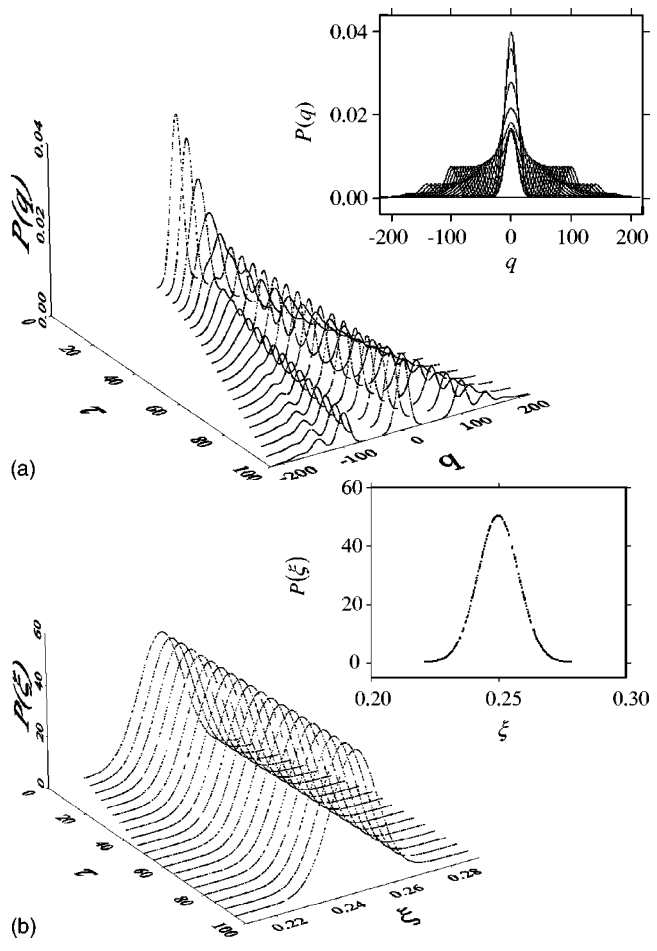

FIG. 7. The time evolution of the atomic wave packet of an infinitely heavy atom free of damping located at a node (a) in momentum space and (b) in coordinate space. The insets are ground-level views into the time axis.

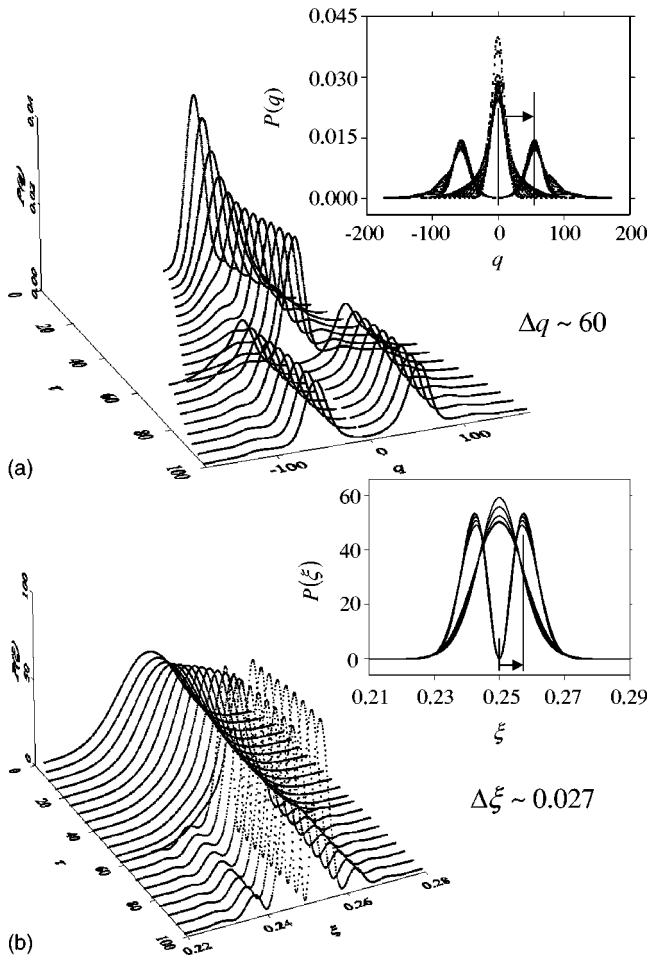

FIG. 8. The dynamics of a wave packet in the presence of damping in which an atomic jump has occurred (a) in momentum space and (b) in coordinate space. $\gamma=0.1$ and $\Delta q=10$, for an *infinitely heavy atom* initially in the ground state placed at a node, with the cavity field in a one-quantum coherent state. The insets are ground-level views along the time axis.

$$\frac{d}{dt}\mathcal{P}(\xi)=\mathcal{P}_0\sum_{n,a}\int dqdq' e^{i2\pi(q-q')\xi}[\dot{C}_a(n,q)C_a^*(n,q') + C_a(n,q)C_a^*(n,q')]. \tag{30}$$

Now from the dynamical equations (17a) and (17b), without the damping term, we have

$$\dot{C}_e(n,q)C_e^*(n,q')=-\frac{\sqrt{n}}{2}[C_g(n,q-1)C_e^*(n,q') + C_g(n,q+1)C_e^*(n,q')], \tag{31a}$$

$$C_g(n,q)\dot{C}_g^*(n,q')=+\frac{\sqrt{n}}{2}[C_g(n,q)C_e^*(n,q'-1) + C_g(n,q)C_e^*(n,q'+1)], \tag{31b}$$

etc., and simply because

$$\int dqdq' e^{i2\pi(q-q')\xi}[-C_g(n,q-1)C_e^*(n,q') + C_g(n,q)C_e^*(n,q'+1)]=0, \tag{32}$$

etc., we find

$$\frac{d}{dt}\mathcal{P}(\xi)=0. \tag{33}$$

Nevertheless, even more interesting things happen when the atom is subject to damping. Then the wave packet of an infinitely massive atom does show dynamical evolutions in *coordinate* space as well both through the coherent decay during the continuous evolution and by atomic jumps. Figures 8(a) and 8(b) show a typical time evolution of a wave packet which has gone through a single atomic jump in momentum space (a) and in coordinate space (b) where $\gamma=0.1$, $\Delta q=10$ and $M=\infty$ for an atom initially in the ground state and the field in a one-quantum coherent state in a lossless cavity. In Fig. 8(b), we clearly see the actual evolution of the

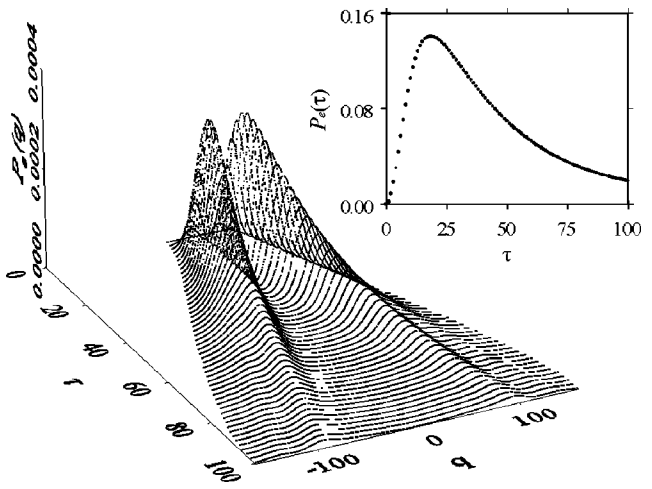

FIG. 9. The evolution of $\mathcal{P}_e(q)=\Sigma_n|C_e(n,q)|^2$. The inset shows the temporal behavior of $P_e=\int dq\mathcal{P}(q)$.

wave packet in coordinate space during the coherent process, not only the drastic change after the atomic jump: The wave packet gets indeed continuously squeezed around its peak. The question is how such a motion of the wave packet of an infinitely heavy atom can occur in coordinate space. The reason that damping causes this type of wave packet evolution even for an infinitely massive atom can be seen in Eqs. (17a) and (17b). There the atomic damping makes the two equations symmetric in the sense that it adds a damping term only in Eq. (17a), and thereby we no longer have identities such as Eq. (32).

Since everything happened for an infinitively heavy atom, the dynamics following an atomic jump is not a mechanical process. That is, the mean position of a peak in coordinate space cannot be related to a time integral of that in momentum space in the fashion $\overline{x}=\int(\overline{p}/M)dt$, as we did in Sec. II, for an obvious reason. The alert reader will find that the correct relation between the mean positions $\overline{x}$ and $\overline{p}$ in both spaces right after an atomic jump is indeed obtained from the uncertainty relation—i.e., $\overline{x}\sim\alpha/\overline{p}$ where α is a constant on the order of $\hbar$, though it is not exactly $\hbar/2$ because the wave packet no longer retains the minimum uncertainty, as Figs. 8(a) and 8(b) demonstrate [33–35]. Thus, it should be entirely attributed to the intrinsic wave nature of a matter article as well as to the issue of the position and momentum uncertainty which forms the very heart of quantum mechanics [36].

C. Overdamped case

When the atomic damping is strong such that $\gamma\geqslant 1$ (out of the strong coupling regime), the wave packet essentially follows the coherent decay only, without quantum jumps. This can be quickly appreciated from the dynamical equations in the quantum trajectory, Eqs. (24a) and (24b). The form of Eq. (24a) shows that the atomic upper-state probability $|C_e(n,q)|^2$ has an early time dependence roughly of the form $\tau^2\exp(-\gamma\tau)$. Figure 9 shows the temporal behaviors of $\mathcal{P}_e(q)=\Sigma_n|C_e(n,q)|^2$ and $P_e=\int dq\mathcal{P}(q)$ in a trajectory in which an atomic jump has not occurred yet. For a large γ, the exponential-type factor dictates so that the atomic upper-state probability quickly decays to zero, having no time to grow up to an appreciable value. Thus no atomic jumps are likely, and the system follows only the coherent decay. While damping tends to put the system back to its initial internal energy state in this fashion, the atom-field momentum exchange process rapidly broadens the wave packet in momentum space, which ends up narrowing—i.e., localizing—the wave packet in coordinate space although the uncertainty product $\Delta x\Delta p$ slowly grows in general. This is none other than the phenomenon of "damping-induced localization" (DIL) [37]. For a moderate atomic damping, the wave packet follows the coherent evolution showing DIL until an atomic jump which brings about a sudden splitting—a gigantic change—in the wave packet as shown in Figs. 8(a) and 8(b).

D. Effect of cavity decay

The cavity quantum jumps, on the other hand, do not do much in the wave packet splitting. To see this let us turn off the atomic damping channel and open the cavity decay channel. Then Eq. (25) is replaced by the process

$$|\overline{\Psi}\rangle\rightarrow a|\Psi\rangle, \tag{34}$$

which brings about changes in the coefficients such that

$$\overline{C}_e^{\tau}(n,q)\rightarrow\sqrt{n}C_e^{\tau}(n+1,q), \tag{35a}$$

$$\overline{C}_g^{\tau}(n,q)\rightarrow\sqrt{n+1}C_g^{\tau}(n+1,q). \tag{35b}$$

It will certainly change the shape of the wave packet slightly, but never as much as splitting the packet into two pieces. Particularly when the mean cavity photon number is high, there will be no essential change, whereas the packet splitting due to the atomic decay is regardless of the intensity of the field.

IV. QUANTUM-TRAJECTORY SIMULATION OF A TYPICAL EXPERIMENT

Since atomic damping changes the wave packet in such a radical fashion, one may expect that it can play a significant role in actual experiments. An actual experimental setup will be most possibly such that a beam of atoms are launched to fly through the cavity mode while the cavity is continuously pumped by an external field, and one measures the position distribution of the atoms emerging from the interaction region on a surface at some distance from the cavity.

For the purpose of particularly watching the effect of damping in the OSGE, one may simplemindedly consider a conditional measurement in which one records the position distribution of only those atoms that have undergone any number of quantum jumps. However, one will soon realize that it will not work that way because, even in such a circumstance, always is there the wave packet splitting due to the coherent process. That is, it seems not practically possible to say, "This much splitting is due to the coherent evolution and that much is due to the quantum jumps." One may then consider another scheme in which the atom-field inter-

action time is set so short that there is negligible splitting via the coherent process, and the aforesaid conditional measurement is done. But then again, one will realize that it is not possible to resolve the splitting right after the jumps because it is within the Heisenberg uncertainty limit. In the region far from the interaction zone, on the other hand, the position distribution gets so broad that the tiny splitting will be completely buried.

So, in this work, we just limited our attention to the question of whether the OSGE discussed so far could be practically observed in a typical cavity-QED experiment even in the presence of appreciable damping strengths. We did a Monte Carlo simulation of a typical cavity-QED experiment using the quantum-trajectory method. Below we will compare the result of a hypothetical experiment in which the atoms are assumed to be nonradiative with that of a realistic experiment in which the atoms are radiative. Obviously the difference will be none other than the effect of atomic damping in the OSGE.

As we did in our previous work on the cavity-QED atom detection system [21], we assumed a single-mode cavity resonant to the transition line of barium (^{138}Ba) atom, $\lambda = 553$ nm, with $g_0/2\pi = 42$ MHz, which correspond to $\mu \sim 1.1 \times 10^{-4}$. The transverse cavity mode is assumed to have a profile so that $g(\vec{x}) = g_0 \exp[-(y^2+z^2)/w^2]\cos kx$, where the cavity axis lies in the x direction and w, the mode waist, is taken to be 37 μm. The atomic longitudinal velocity is set to $v_z = 400$ m/sec. The driving field amplitude $\mathcal{E}$ is such that $\mathcal{E}/\kappa = 1$ so that the mean intracavity photon number is just 1 at steady state—i.e., $\langle a^\dagger a \rangle_{ss} = 1$—before the entry of an atom. We choose damping strengths as large as $\gamma/g_0 = 2\kappa/g_0 = 0.5$. We assume that the initial atomic wave packet, to be determined by the geometry of the system, is a Gaussian having momentum uncertainty $\Delta p = 10\hbar k$ which again corresponds to $\Delta x \leqslant \lambda/100$, a well-localized, particle like wave packet. Note that the "initial time" is the time when the atoms reach the plane normal to the atomic path, assumed to be at $10w$ away, for instance, from the cavity axis. Thus, until the wave packet reaches the region of appreciable atom-field coupling strength, it will freely evolve.

Figure 10 shows the "far-field" momentum distributions averaged over 300 atoms detected on a screen located at a large distance—approximately $40w$ away, for instance, from the cavity axis. (Note that the far-field position distributions are exactly the same in shape as those of the momentum distributions with proper axis labeling and scaling, according to the diffraction theory.) Let us add that it took about a month for our 16-node PC cluster of clock speed 2.4 GHz to complete the computation of 300 quantum trajectories only to obtain this figure. The thinner line is for case (a) in which the atoms are assumed to be nonradiative, while the thicker is for case (b) where the atomic decay channel is let open with $\gamma/g_0 = 0.5$. It turns out that during the entire flight time, each atom has gone through about 25 jumps on average in case (b). The figure shows that, even for the atoms and cavity as strongly damped as the given strengths, the wave packet splitting robustly shows up, having hardly been washed out. The overall width of $\mathcal{P}(q)$ in case (a) is greater than the value in case (b), the height of $\mathcal{P}(0)$ in case (a) being smaller than

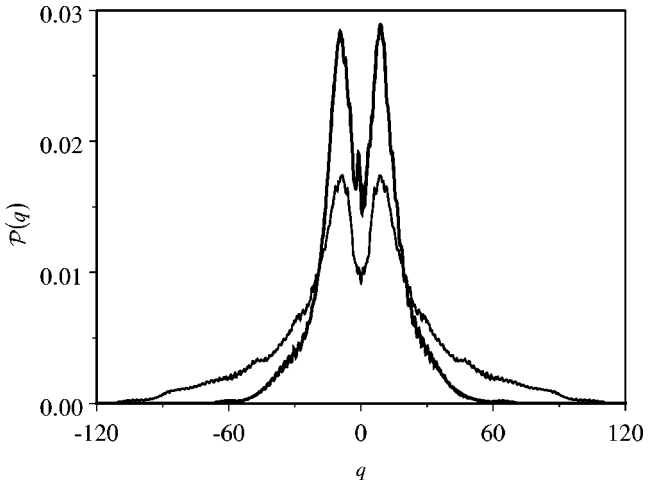

FIG. 10. The "far-field" momentum distributions averaged over 300 atoms at a location approximately $40w$ away from the cavity axis. The thinner line is for the case of nonradiative atoms, while the thicker line is for the case of radiative atoms with $\gamma/g_0 = 0.5$.

that in case (b). The narrower distribution of case (b) can be interpreted as weaker diffusive motion of the atoms in the field during the interaction time. Less diffusion implies less frequent exchanges of quanta between the atom and field—i.e., a weaker interaction. So the mean-field intensity is smaller in the latter case, which again indicates a greater portion of the vacuum state in the cavity field on average. The stronger contamination of the cavity field by the vacuum state is due to the introduction of an additional damping channel—i.e., the atomic damping—to the system. The narrower width in case (b) can be understood in this way which may be another interpretation of DIL.

Let us wrap up this section by leaving with a brief remark on the states of the detected atoms: Without atomic damping, the outcome of such an experiment would also yield the wave packet split into a pair of distinct bumps like the thin line in Fig. 10. Then each bump will correspond to the aggregate of atoms in either of the orthogonal dressed states. If atomic damping is present, however, things become different. Note that an atomic jump will put the atom back to its ground state which is simply a 50-50 mixture of the orthogonal dressed states. Furthermore, the final state of the system will eventually decay into the product of the atomic ground state and the initial coherent field state such that

$$\lim_{t\to\infty} |\Psi(t)\rangle = |\psi_f\rangle \otimes |\psi_a\rangle = |\alpha\rangle \otimes \int dp C(p) |p,g\rangle, \quad (36)$$

where $\alpha = \mathcal{E}/\kappa$, since the atom-field entanglement gets lost as the cavity field is restored to the initial state by the driving field whereas the atom eventually decays into the ground state. Thus the atomic states on both peaks are the same. So, when atomic damping is present, it is difficult to say that the state on one peak is, or has been, orthogonal to that on the other.

V. SUMMARY

We analyzed the optical Stern-Gerlach effect in the cavity-QED realm. We presented an intuitive interpretation

of the optical Stern-Gerlach effect in the dressed-state picture. We particularly investigated the effect of atomic damping on the wave packet evolution in the framework of quantum-trajectory theory. In the viewpoint of QTT, it is found that the atomic damping can also cause the wave packet splitting, and furthermore this process occurs in a *nonmechanical* fashion, as opposed to the coherent process that is *mechanical*. It is also found that the *continuous* atomic decay process tends to localize the atomic wave packet, keeping it from spreading so fast as in the case of no atomic damping, whereas the *discontinuous* atomic jumps tend to split the packet. Proposing a feasible experimental scheme in the cavity-QED realm, we pointed out that the phenomenon of atomic wave packet splitting could be experimentally observed, even in a moderate coupling regime where the atomic damping rate is comparable to the atom-field coupling constant.

ACKNOWLEDGMENT

This work was supported by Korea Research Foundation Grant No. KRF-2002-070-C00044.

[1] P. L. Kapitza and P. A. M. Dirac, Proc. Cambridge Philos. Soc. **29**, 297 (1933).
[2] P. Meystre, E. Schumacher, and S. Stenholm, Opt. Commun. **73**, 443 (1989).
[3] P. L. Gould, P. J. Martin, G. A. Ruff, R. E. Stoner, J.-L. Picqué, and D. E. Pritchard, Phys. Rev. A **43**, 585 (1991); P. E. Moskowitz, P. L. Gould, S. R. Atlas, and D. E. Pritchard, Phys. Rev. Lett. **51**, 370 (1983).
[4] S. M. Tan and D. F. Walls, Phys. Rev. A **44**, R2779 (1991).
[5] S. Kunze, K. Dieckmann, and G. Rempe, Phys. Rev. Lett. **78**, 2038 (1997).
[6] B. Shore, P. Meystre, and S. Stenholm, J. Opt. Soc. Am. B **8**, 903 (1991).
[7] Kyungwon An, Young-Tak Chough, and Sun-Hyun Youn, Phys. Rev. A **62**, 023819 (2000).
[8] *Atom Interferometry*, edited by P. R. Berman (Academic, San Diego, 1997).
[9] J. Opt. Soc. Am. B (1987), special issue on laser cooling and trapping, edited by V. Bagnato, N. Bigelow, A. Dykhne, J. Weiner, and Y. Yakovlev; J. Opt. Soc. Am. B **6** (11) (1989), special issue on laser cooling and trapping of atoms, edited by S. Chu and C. Wiseman.
[10] P. W. H. Pinkse, T. Fischer, P. Maunz, and G. Rempe, Nature (London) **404**, 365 (2000).
[11] C. J. Hood, T. W. Lynn, A. C. Doherty, A. S. Parkins, and H. J. Kimble, Science **287**, 1447 (2000).
[12] H. Walther, Nature (London) **414**, 49 (2001).
[13] R. J. Cook, Phys. Rev. Lett. **41**, 1788 (1978).
[14] C. Tanguy, S. Reynaud, and C. Cohen-Tannoudji, J. Phys. B **17**, 4623 (1984).
[15] A. P. Kazantsev, Sov. Phys. JETP **40**, 825 (1975); Sov. Phys. Usp. **21**, 58 (1978).
[16] T. Sleator, T. Pfau, V. Balykin, O. Carnal, and J. Mlynek, Phys. Rev. Lett. **68**, 1996 (1992).
[17] W. Gerlach and O. Stern, Z. Phys. **8**, 110 (1922).
[18] P. Meystre, E. Schumacher, and S. Stenholm, Opt. Commun. **73**, 443 (1989).
[19] A. Vaglica, Phys. Rev. A **54**, 3195 (1996); **58**, 3856 (1998).
[20] A. M. Ishkhanyan, Phys. Rev. A **61**, 063611 (2000).
[21] Young-Tak Chough, Sun-Hyun Youn, Hyunchul Nha, Sang Wook Kim, and Kyungwon An, Phys. Rev. A **65**, 023810 (2002).
[22] A. M. Herkommer, V. M. Akulin, and W. P. Schleich, Phys. Rev. Lett. **69**, 3298 (1992).
[23] M. Freyberger and A. M. Herkommer, Phys. Rev. Lett. **72**, 1952 (1994).
[24] I. Sh. Averbukh, V. M. Akulin, and W. P. Schleich, Phys. Rev. Lett. **72**, 437 (1994).
[25] P. Domokos, P. Adam, J. Janszky, and A. Zeilinger, Phys. Rev. Lett. **77**, 1663 (1996).
[26] H. J. Carmichael, *An Open Systems Approach to Quantum Optics* (Springer, Berlin, 1993).
[27] Young-Tak Chough, Keon-Kee Kim, Hyunchul Nha, Jai-Hyung Lee, Kyungwon An, and Sun-Hyun Youn, J. Korean Phys. Soc. **42**, 106 (2003).
[28] J. Dalibard and C. Cohen-Tannoudji, J. Opt. Soc. Am. B **2**, 1707 (1985).
[29] One may be concerned that restricting the atoms to a Gaussian slit of a mere few nanometers ($\lambda/100$) would make the available atomic flux extremely small. However, in our recent atomic beam experiments, we have obtained an atomic flux of 10^{13} atoms/(sec cm^2) with a 3% velocity spread around the mean of about 700 m/sec. Suppose we place a slit with a horizontal width of $\lambda/100$ in front of the cavity in order to localize the initial atomic position. Since the cavity mode in our example has a mode waist of 37 μm, the vertical width of the slit can be as wide as 37 μm (about 20λ), still offering a uniform coupling constant. This area with the above atomic flux gives about 5000 atoms/sec through the slit which is not a small number at all.
[30] B. Rohwedder and M. Orszag, Phys. Rev. A **54**, 5076 (1996).
[31] C. W. Gardiner, *Quantum Noise* (Springer-Verlag, Berlin, 1991).
[32] H. J. Carmichael, *Statistical Methods in Quantum Optics I* (Springer-Verlag, Berlin, 1999).
[33] E. T. Jaynes and F. W. Cummings, Proc. IEEE **51**, 89 (1963).
[34] J. H. Eberly, N. B. Narozhny, and J. J. Sanchez-Mondragon, Phys. Rev. Lett. **44**, 1323 (1980).
[35] *Cavity Quantum Electrodynamics*, edited by P. R. Berman (Academic, Boston, 1994).
[36] This type of nonmechanical aspect in quantum-mechanical processes might have been one of the reasons why David Bohm used to call quantum mechanics "quantum *non*-mechanics." See David Bohm, *Quantum Theory* (Dover, New York, 1989), p. 167.
[37] See, e.g., B. M. Garraway and P. L. Knight, in *Quantum Optics VI*, edited by J. D. Harvey and D. F. Walls, Springer Proceedings in Physics Vol. 77 (Springer, Berlin, 1994), p. 173, and the references therein.